

1 **Physically-based Assessment of Hurricane Surge Threat under Climate Change**

2 Ning Lin^{1*}, Kerry Emanuel¹, Michael Oppenheimer², Erik Vanmarcke³

3

4 ¹Department of Earth, Atmospheric, and Planetary Sciences, Massachusetts Institute of
5 Technology, Cambridge, MA 02139-4307, USA

6 ²Department of Geosciences and the Woodrow Wilson School, Princeton University, Princeton,
7 NJ 08544, USA

8 ²Department of Civil and Environmental Engineering, Princeton University, Princeton, NJ 08544,
9 USA

10

11 *Corresponding author, ninglin@mit.edu

12

13

14

15

16

17

18

19

20

21 **Abstract**

22 Storm surges are responsible for much of the damage and loss of life associated with landfalling
23 hurricanes. Understanding how global warming will affect hurricane surge thus holds great
24 interest. As general circulation models (GCMs) cannot simulate hurricane surges directly, we
25 couple a GCM-driven hurricane model with hydrodynamic models to simulate large numbers of
26 synthetic surge events under projected climates and assess surge threat, as an example, for New
27 York City (NYC). Struck by several intense hurricanes in recorded history, NYC is highly
28 vulnerable to storm surges. We show that the surge level for NYC will likely increase due to the
29 change of storm climatology with a magnitude comparable to the projected sea-level rise (SLR),
30 based on some GCMs. The combined effects of storm climatology change and a 1-m SLR may
31 cause the current NYC 100-year surge flooding to occur every 3-20 years and the 500-year
32 flooding to occur every 25-240 years by the end of the century.

33

34 **Introduction**

35 Associated with extreme winds, rainfall, and storm surges, tropical cyclones present major
36 hazards for coastal areas. Moreover, tropical cyclones respond to climate change^{1, 2, 3}. Previous
37 studies predicted an increase in the global mean of the maximum winds and rainfall rates of
38 tropical cyclones in a warmer climate⁴; however, the effect of climate change on storm surges,
39 the most damaging aspect of tropical cyclones, remains to be investigated⁴. Hurricane Katrina of
40 2005, the costliest natural disaster in U.S. history, produced the greatest coastal flood heights
41 ever recorded in the U.S., causing more than \$100 billion in losses and resulting in about 2000
42 fatalities. On the eastern U.S. coast, where tropical cyclones are less frequent than in the Gulf of
43 Mexico and Florida regions, the Great Hurricane of 1938 produced record flood heights in Long

44 Island and southern New England, killing 600-800 people. A question of increasing concern is
45 whether such devastating surge events will become more frequent.

46

47 The storm surge is a rise of water driven by a storm's surface wind and pressure gradient forces
48 over a body of shallow water; its magnitude is determined, in a complex way, by the
49 characteristics of the storm plus the geometry and bathymetry of the coast. As a result, the
50 change of surge severity cannot be inferred directly from the change of storm intensity^{5, 6, 7, 8}.

51 For example, Hurricane Camille of 1969 (Category 5) made landfall in the same region of
52 Mississippi as the less intense Hurricane Katrina (Category 3), but produced lower surges due to
53 its smaller size^{5,6,9}. Using only a storm's landfall characteristics to predict surges is also
54 inaccurate^{10, 11}, as the evolution of the storm before and during landfall affects the surge.

55 Furthermore, similar storms can produce quite different surges at locations with different
56 topological features⁶. Therefore, quantifying the impact of climate change on hurricane surges
57 requires explicit modeling of the development of storms and induced surges at local scales under
58 projected climates.

59

60 Modeling hurricane surges under climate scenarios, however, is not straightforward, because
61 tropical cyclones cannot be resolved in current GCMs due to their relatively low resolution
62 (~100 km) compared to the size of storm core (~ 5 km). Although high-resolution regional
63 models (e.g., refs 12 and 13) may be used to downscale the GCM simulations, these models are
64 still limited in horizontal resolution and are too expensive to implement for risk assessment. This
65 study takes a more practical approach, coupling a simpler GCM-driven statistical/deterministic

66 hurricane model with hydrodynamic surge models to simulate cyclone surges for different
67 climates.

68

69 Computationally efficient, this method can be used to generate large numbers of synthetic surge
70 events at sites of interest, providing robust statistics to characterize surge climatology and
71 extremes. We apply this method to investigate current and future hurricane surge threat for NYC,
72 considering also the contribution of wave setup, astronomical tides, and SLR. The resulting surge
73 flood return-level curves provide scientific bases for climate adaptation and sustainable
74 development in rapidly developing coastal areas^{14,15,16}.

75

76 **Storm simulation**

77 The statistical/deterministic hurricane model^{17, 18} used in this study generates synthetic tropical
78 cyclones under given large-scale atmospheric and ocean environments, which may be estimated
79 from observations or climate modeling. This method does not rely on the limited historical track
80 database, but rather generates synthetic storms that are in statistical agreement with
81 observations¹⁷, and it compares well with various other methods used to study the effects of
82 climate change on tropical cyclones^{18, 19,4}. In this study, we assume the cyclone-threatened area
83 for NYC to be within a 200-km radius from the Battery (74.02 W, 40.9 N; chosen as the
84 representative location for NYC), and we call it a NY-region storm if a storm ever passes within
85 this threatened area with a maximum wind speed greater than 21 m/s. To investigate the current
86 surge probabilities, we generate a set of 5000 NY-region storms under the observed climate
87 (represented by 1981-2000 statistics) estimated from the National Center for Environmental
88 Prediction/National Center for Atmospheric Research (NCAR/NCEP) reanalysis²⁰. To study the

89 impact of climate change, we apply each of four climate models, CNRM-CM3 (Centre National
90 de Recherches Météorologiques, Météo-France), ECHAM5 (Max Planck Institution), GFDL-
91 CM2.0 (NOAA Geophysical Fluid Dynamics Laboratory), and MIROC3.2
92 (CCSR/NIES/FRCGC, Japan), to generate four sets of 5000 NY-region storms under current
93 climate conditions (1981-2000 statistics) and another four sets of 5000 NY-region storms under
94 future climate conditions (2081-2100 statistics) for the IPCC-AR4 A1B emission scenario²¹.
95 (Most of the climate data are obtained from the World Climate Research Program (WCRP) third
96 Climate Model Intercomparison Project (CMIP3) multimodel dataset.) We choose these four
97 climate models because, based on the study of ref. 18, the predictions of the changes in storm
98 frequency, intensity, and power dissipation in the Atlantic basin by these models span the range
99 of predictions by all seven CMIP3 models from which the required model output is available.

100

101 The annual frequency of the historical NY-region storms is estimated from the best-track
102 Atlantic hurricane dataset (updated from ref. 22) to be 0.34; we assume this number to be the
103 storm annual frequency under the current climate. Since the hurricane model does not produce an
104 absolute rate of genesis, the storm frequency derived from each climate model for the current
105 climate is calibrated to the observed value (0.34), and the frequency for the future climate is then
106 predicted¹⁸. Estimated annual frequencies of future NY-region storms from the four climate
107 models differ: CNRM is 0.7, ECHAM is 0.3, GFDL is 1.34, and MIROC is 0.29; the change of
108 the storm frequency due to global warming ranges from a decrease of 12% to an increase of
109 290%. The large variation among the model predictions reflects the general uncertainties in
110 climate models' projections of tropical cyclone frequency, due to systematic model differences
111 and internal climate variability (which may not be averaged out over the 20-yr periods

112 considered here¹⁸). According to ref. 23, as much as half of the uncertainty may be owing to the
113 climate variability. Moreover, the variations in the projected storm frequency changes at global
114 or basin scales, as in refs. 4 and 18, are greatly amplified at local scales, as in this study, due to
115 the differences in the storm track and intensity changes predicted by the climate models. We also
116 note that even larger variations in the storm frequency changes can be induced if more climate
117 models are considered; for example, the Hadley Center UK Meteorological Office model
118 UKMO-HadCM3 may predict a relatively large reduction in the storm frequency due to climate
119 change, based on the study of ref. 3.

120

121 **Surge modeling**

122 This study uses two hydrodynamic models: the Advanced Circulation Model (ADCIRC^{24, 25})
123 and the Sea, Lake, and Overland Surges from Hurricanes (SLOSH²⁶) model, both of which have
124 been validated and applied to simulate storm surges and make forecasts for various coastal
125 regions (e.g., refs 27, 28, 29, 30, 31, 32). Storm surges are driven by storm surface wind and
126 sea-level pressure fields. For the ADCIRC simulations, the surface wind (10-min. average at 10
127 m) is estimated by calculating the wind velocity at the gradient height with an analytical
128 hurricane wind profile³³, translating the gradient wind to the surface level with a velocity
129 reduction factor (0.85³⁴) and an empirical expression of inflow angles³⁵, and adding a fraction
130 (0.5; based on observed statistics) of the storm translation velocity to account for the asymmetry
131 of the wind field; the surface pressure is estimated from a parametric pressure model³⁶. For the
132 SLOSH simulations, the wind and pressure are determined within the SLOSH model by a semi-
133 parametric hurricane model²⁶. The two hydrodynamic models are applied with numerical grids of
134 various resolutions (from ~1 km to ~ 10 m around NYC). The SLOSH simulation with a coarse

135 resolution grid is used to select the extreme surge events, which are further analyzed with higher-
136 resolution ADCIRC simulations to estimate the probability distributions of NYC surges (see
137 Methods and Supplementary Figs. S1 and S2).

138
139 As examples, Figure 1 displays the spatial distribution of the storm surge around the NYC area
140 for two worst-case scenarios for the Battery under the NCAR/NCEP current climate. The storm
141 that generates the highest surge (4.75 m) at the Battery moves northeastward and close to the site
142 with a high intensity (Fig. 1a). A relatively weaker storm that moves farther from the site also
143 produces a comparable surge (4.57 m) at the Battery, due to its larger size and northwestward
144 translation (Fig. 1b). Both storms pass to the west of the Battery, inducing high surges at the site
145 with their largest wind forces to the right of the track; this effect (of the wind field's asymmetry)
146 on the surge is particularly significant for northwestward-moving storms, which concentrate their
147 strongest wind forces on pushing water into New York Harbor and up to lower Manhattan. These
148 two worst-case surges for the Battery have very low occurrence probabilities under the current
149 climate condition. However, NYC has indeed been affected by numerous intense storm surges in
150 recorded history and, based on the local sedimentary evidence, prehistory³⁷. The highest water
151 level at the Battery as inferred from historic archives was about 3.2 m relative to the modern
152 mean sea level, due to a hurricane in 1821 striking NYC at a low tide³⁷; thus the largest historical
153 surge at the Battery might be about 3.8 m (given the magnitude of the local low tide of about 0.5-
154 0.8 m).

155
156 We also investigate the influences of other processes related to the surge for NYC, using a set of
157 over 200 most extreme surge events. To investigate the effects of wave setup, we simulate the

158 extreme events with the ADCIRC model coupled with a wave model³²; the wave setup is found
159 to be relatively small for the study region (see Fig. S3), and thus it is neglected in our estimation
160 of surge probabilities. We notice, however, that the nonlinear effect of the astronomical tide on
161 the surge (tide-surge nonlinearity) is relatively large (see Fig. S4). We model this nonlinearity as
162 a function of the surge and tidal characteristics, based on a database generated for the extreme
163 events (see Methods and Fig. S5). This function is then used to estimate the storm tide as a
164 combination of the surge and astronomical tide. In addition, we study the nonlinear effect on the
165 surge from the SLR, by simulating the extreme surges for a range of projected SLRs for NYC.
166 This SLR effect is found to be negligible (see Fig. S6), and thus projected SLRs in future
167 climates are accounted for linearly in the estimation of the flood height for NYC.

168

169 **Statistical analysis**

170 We assume the annual number of NY-region storms to be Poisson-distributed (see Fig. S7), with
171 as mean the annual storm frequency. For each storm arrival, the probability density function
172 (PDF) of the induced surge is estimated from the generated surge database. Our empirical
173 datasets show that the surge PDF is characterized by a long tail, which determines the risk. We
174 apply a Peaks-Over-Threshold (POT) method to model this tail with a Generalized Pareto
175 Distribution (GPD), using the maximum likelihood method, and the rest of the distribution with
176 non-parametric density estimation. The GPD fits relatively well with the surge distribution for
177 almost all storm sets in this study (Figs. S8 and S9). The estimated storm frequency and surge
178 PDF are then combined to generate the surge return-level curves and associated statistical
179 confidence intervals (calculated with the Delta method³⁸). The surge PDF is further applied to
180 estimate the storm tide and flood height return levels (see Methods).

181

182 **Current surge threat**

183 The estimated return levels of the storm surge at the Battery under the NCAR/NCEP current
184 climate appear in Fig. 2. The estimated current 50-year storm surge is about 1.24 m, the 100-year
185 surge is about 1.74 m, and the 500-year surge is about 2.78 m. A previous study³⁹, using the
186 SLOSH model with a relatively coarse mesh, predicted a higher surge (2.14 m) for the 100-year
187 return period but lower surges for longer return periods (e.g., 2.73 m for the 500-year surge) for
188 this site. These differences result mainly from the different wind profiles and grid resolutions
189 applied in the ADCIRC and SLOSH simulations and the different storm sets (statistical samples)
190 used. The estimated return level of the storm tide, shown also in Fig. 2, is about 0.3-0.5 m higher
191 than the storm surge level. Thus, the estimated current 50-year storm tide is about 1.61 m, the
192 100-year storm tide is about 2.03 m, and the 500-year storm tide is about 3.12 m. Considering
193 that much of the seawall protecting lower Manhattan is only about 1.5 m above the mean sea
194 level³⁰, NYC is presently highly vulnerable to extreme hurricane-surge flooding. For return
195 periods under 50 years, extratropical cyclones may also contribute to the coastal flooding risk
196 and become the main source of 1-10 year coastal floods for NYC^{40, 41}.

197

198 **Impact of climate change**

199 The predictions of storm tide return levels for current and future IPCC A1B climates are
200 presented in Fig. 3. (In the context of climate change, the return level at period T may be
201 understood as the level with an annual exceedance probability of $1/T$.) The results from the four
202 climate models differ: CNRM predicts an increase of the storm tide level, while ECHAM

203 predicts a decrease; GFDL predicts that the storm tide level will increase for the main range of
204 the return period but decrease for very long return periods, while MIROC predicts a decrease for
205 low and moderate return periods but an increase for longer return periods. However, the
206 magnitudes of the changes (the ratio of A1B to the current-climate levels) using CNRM (1.13-
207 1.24) and GFDL (0.98-1.44) are more significant than those using ECHAM (0.89-0.96) and
208 MIROC (0.89-1.08). The discrepancies among the model results can be attributed to the models'
209 different estimations of the change of the storm frequency and the surge severity. The storm
210 frequency on a local scale plays an important role in determining the surge risk; the prediction of
211 the frequency change for NY-region storms by the four climate models varies greatly. Moreover,
212 unlike the average storm intensity, which is predicted to increase by these and other climate
213 models⁴, the storm surge severity is predicted to increase by some models but decrease by others.
214 This difference appears because the surge magnitude depends on other parameters of the storm
215 as well as on its intensity, all of which may change differently in the different climate models.

216

217 We suspect that a main reason that the increase of storm intensity (in some models) does not
218 translate to an increase in surge magnitude is that the storm's radius of maximum wind (R_m)
219 tends to decrease as the storm intensity increases, given the assumption made in the above
220 simulations that the distribution of the storm's outer radius (R_o , determined from observed
221 statistics⁴²) remains the same under different climates. However, in theory the storm's overall
222 dimension scales linearly with the potential intensity⁴³; therefore, the increase of potential
223 intensity in a warmer climate⁴⁴ may induce an increase of R_o . Consequently, the reduction of R_m
224 due to the increase of storm intensity may be offset and even reversed. In such a case, climate
225 change will likely increase storm intensity and size simultaneously, resulting in a significant

226 intensification of storm surges. In order to test this hypothesis, we performed the simulations as
227 before but assumed that R_o increases by 10% and R_m increases by 21% in the future climate. We
228 base this assumption on the estimated change of the potential intensity in the future climate
229 (expected to increase by about 10%⁴) and on a theoretical scaling relationship between R_o and R_m
230 (R_m scales with R_o^2)³³. The storm tide level thus predicted, shown also in Fig. 3, is higher or
231 nearly unchanged in the future climate for the four models. The magnitude of the change also
232 grows due to the increase of the storm size; it becomes 1.23-1.36 for CNRM, 1.05-1.50 for
233 GFDL, 0.95-1.02 for ECHAM, and 0.97-1.11 for MIROC. At present, the effect of climate
234 change on hurricane size has not been investigated; therefore, it is unclear whether the surge will
235 greatly increase due to the simultaneous increase in storm intensity and size or only moderately
236 change when one factor increases while the other decreases. Further investigation of the storm
237 size distribution under different climates is needed to answer this question.

238

239 Discussion

240 As the climate warms, the global mean sea level is projected to rise, due to thermal expansion
241 and melting of land ice. Superimposed on the global SLR, regional sea levels may change due to
242 local land subsidence and ocean circulation changes, both of which are expected to significantly
243 increase sea level in the NYC area^{45, 46}. The total SLR for NYC is projected to be in the range of
244 0.5-1.5 m by the end of the century^{21, 40, 47}. The effect of SLR, rather than changes in storm
245 characteristics, has been the focus of most studies on the impact of climate change on coastal
246 flooding risk (e.g., refs. 45 and 48); some studies also account for the change of hurricane
247 intensity due to the change of the sea surface temperature (e.g., refs. 49 and 50). To our
248 knowledge, this paper is the first to explicitly simulate large numbers of hurricane surge events

249 under projected climates to assess surge probability distributions. Our study shows that some
250 climate models predict the increase of the surge flooding level due to the change of storm
251 climatology to be comparable to the projected SLR for NYC. For example, the CNRM and
252 GFDL models predict that, by the end of the century, the 100-year and 500-year storm tide levels
253 will increase by about 0.7-1.0 m (Figs. 3a and 3c). More consequential, the combined effect of
254 storm climatology change and SLR will greatly shorten the surge flooding return periods. As
255 shown by the estimated flood return level in Fig. 4, if we assume the SLR in the NYC area to be
256 1 m, by the end of the century, the current NYC 100-year surge flooding may occur every 20
257 years or less (with CNRM, GFDL, ECHAM, and MIROC yielding predictions of 4/4, 3/3, 21/20,
258 and 14/13 years, respectively, for observed/increased storm sizes), the current 500-year surge
259 flooding may occur every 240 years or less (with CNRM, GFDL, ECHAM, and MIROC
260 yielding predictions of 62/29, 28/24, 188/140, and 241/173 years, respectively). These findings
261 are dependent on the climate models used to generate the environmental conditions for the storm
262 simulations, so other climate models may produce different results. Nevertheless, all four climate
263 models used in this study predict significant increases in the surge flood level due to climate
264 change, providing an additional rationale for a comprehensive approach to managing the risk of
265 climate change, including long-term adaptation planning and greenhouse-gas emissions
266 mitigation.

267

268 **Methods**

269 High-resolution surge simulations are computationally intensive; therefore, to make it possible to
270 simulate surges with reasonable accuracy for our large synthetic storm sets, we apply the two

271 hydrodynamic models with numerical grids of various resolutions in such a way that the main
272 computational effort is concentrated on the storms that determine the risk of concern. First, the
273 SLOSH simulation, using a polar grid with resolution of about 1 km around NYC, is applied as a
274 filter to select the storms that have return periods, in terms of the surge height at the Battery,
275 greater than 10 years, the typical range of hurricane surge periodicity relevant to design and
276 policy-making. Second, the ADCIRC simulation, using an unstructured grid with resolution of
277 ~100 m around NYC (and up to 100 km over the deep ocean), is applied to each of the selected
278 storms (see Supplementary Fig. S1, for a comparison between SLOSH and ADCIRC
279 simulations). To determine whether the resolution of the ADCIRC simulation is sufficient,
280 another ADCIRC mesh³⁰ with resolution as high as ~10 m around NYC is used to simulate over
281 200 most extreme events under the observed climate condition. The differences between the
282 results from the two grids are very small, with our ~100-m mesh overestimating the surge at the
283 Battery by about 2.5% (Fig. S2). Thus, the ~100-m ADCIRC simulations are used, with a 2.5%
284 reduction, to estimate the surge levels at the Battery for return periods of 10 years and longer.
285 (ADCIRC model control parameters follow refs. 29 and 30, whose results have been validated
286 against observations.)

287
288 To quantify tide-surge nonlinearity, we generate a database of the storm surge and storm tide for
289 over 200 most extreme events arriving every 3 hours during a tidal cycle. We model the
290 nonlinearity (denoted by L : the difference between simulated storm tide, surge, and astronomical
291 tide) as a function of the tidal phase (φ) when the (peak) surge arrives, the surge height (H), tidal
292 range (t_r), and mean tidal level (t_m). We define a non-dimensional factor γ for the nonlinearity as

$$293 \quad \gamma = \frac{L+t_m}{H+t_r}, \quad (1)$$

294 so that, for a given value of γ , the higher the storm surge or the astronomical tide, the larger the
 295 nonlinearity relative to the negative mean tidal level ($-t_m$; considering that the nonlinearity and
 296 the tide are out of phase, Fig. S4). We use the generated storm surge and storm tide database to
 297 estimate γ by kernel regression as a function of the tidal phase (Fig. S5). Then, the nonlinearity
 298 L , for a given tide and a surge H corresponding to tidal phase φ , is estimated as

$$L(\varphi) = \gamma(\varphi)(H + t_r) - t_m. \quad (2)$$

300
 301 We assume the annual number of NY-region storms to be Poisson-distributed, with mean λ .

302 The probability distribution of surge height H , $P\{H < h\}$, is estimated from the generated surges
 303 for each storm set. The surge PDF is applied to estimate the PDF of the storm tide (H^t),

$$P\{H^t < h\} = P\{H + t(\Phi) + L(\Phi) < h\} \quad (3)$$

304 where t is the height of the astronomical tide and Φ is the (random) phase when the storm surge
 305 arrives. Making use of the estimated γ function, equation (3) becomes

$$P\{H^t < h\} = \int_0^{2\pi} P\left\{H < \frac{h - t(\varphi) - \gamma(\varphi)t_r + t_m}{1 + \gamma(\varphi)}\right\} P\{\Phi = d\varphi\}, \quad (4)$$

308 It is reasonable to assume that the surge can happen at any time during a tidal cycle with
 309 equal likelihood, and equation (4) becomes

$$P\{H^t < h\} = \int_0^{2\pi} P\left\{H < \frac{h - t(\varphi) - \gamma(\varphi)t_r + t_m}{1 + \gamma(\varphi)}\right\} \frac{1}{2\pi} d\varphi. \quad (5)$$

311 (Note that equation (5) can be extended to include the effects of different tides during the
 312 hurricane season by taking a weighted average of $P\{H^t < h\}$ for all types of tides considered,
 313 with weights equal to the fractions of time during the season when different types of tide
 314 occur.) Then, by definition, storm tide return period T^t is

$$T^t = \frac{1}{1 - e^{-\lambda(1 - P\{H^t < h\})}}. \quad (6)$$

316 No analytical expression for the return level (h) is available in this case; the storm tide return
 317 levels in Figs. 2 and 3 are calculated by solving equations (5) and (6) numerically. We used the
 318 astronomical tide cycle observed at the site during the period of Sep. 18-19, 1995 (NOAA tides
 319 and currents), assuming the tidal variation at NYC during the hurricane season is relatively
 320 small.

321

322 The surge PDF is also applied to estimate the PDF of the flood height (H^f),

$$323 \quad P\{H^f < h\} = P\{H + t(\Phi) + L(\Phi) + S < h\}, \quad (7)$$

324 where S is the SLR, and the nonlinear effect of SLR on the surge is neglected. Then, based on
 325 equation (5),

$$326 \quad P\{H^f < h\} = \int_0^{s_m} \int_0^{2\pi} P\left\{H < \frac{h-t(\varphi)-\gamma(\varphi)t_r+t_m-s}{1+\gamma(\varphi)}\right\} P\{S = ds\} \frac{1}{2\pi} d\varphi, \quad (8)$$

327 where it is assumed that the range of possible SLR is $[0, s_m]$. The probability distribution of SLR
 328 may be estimated from GCM simulations and/or other methods^{21, 47}. It is also useful to estimate
 329 the flood return level for a certain SLR. For a given SLR (s), equation (8) reduces to

$$330 \quad P\{H^f < h\} = \int_0^{2\pi} P\left\{H < \frac{h-t(\varphi)-\gamma(\varphi)t_r+t_m-s}{1+\gamma(\varphi)}\right\} \frac{1}{2\pi} d\varphi. \quad (9)$$

331 The flood return period T^f is

$$332 \quad T^f = \frac{1}{1 - e^{-\lambda(1-P\{H^f < h\})}}. \quad (10)$$

333 The flood return levels in Fig. 4 are calculated by solving equations (9)-(10) numerically,
 334 assuming a SLR of 1 m ($s=1$) for the future climate (and $s=0$ for the current climate) and using
 335 the astronomical tide cycle observed during Sep. 18-19, 1995. The statistical confidence interval
 336 of the estimated storm tide and surge flood return levels remains the same as the confidence
 337 interval of the estimated surge return level, as no new distribution parameters are introduced. The

338 uncertainty in the estimation of the future return levels may be considered as the combination of
339 the statistical confidence interval and the variation of predictions from different climate models.

340

341 **Please contact Ning Lin (ninglin@mit.edu) for correspondence and requests for materials.**

342

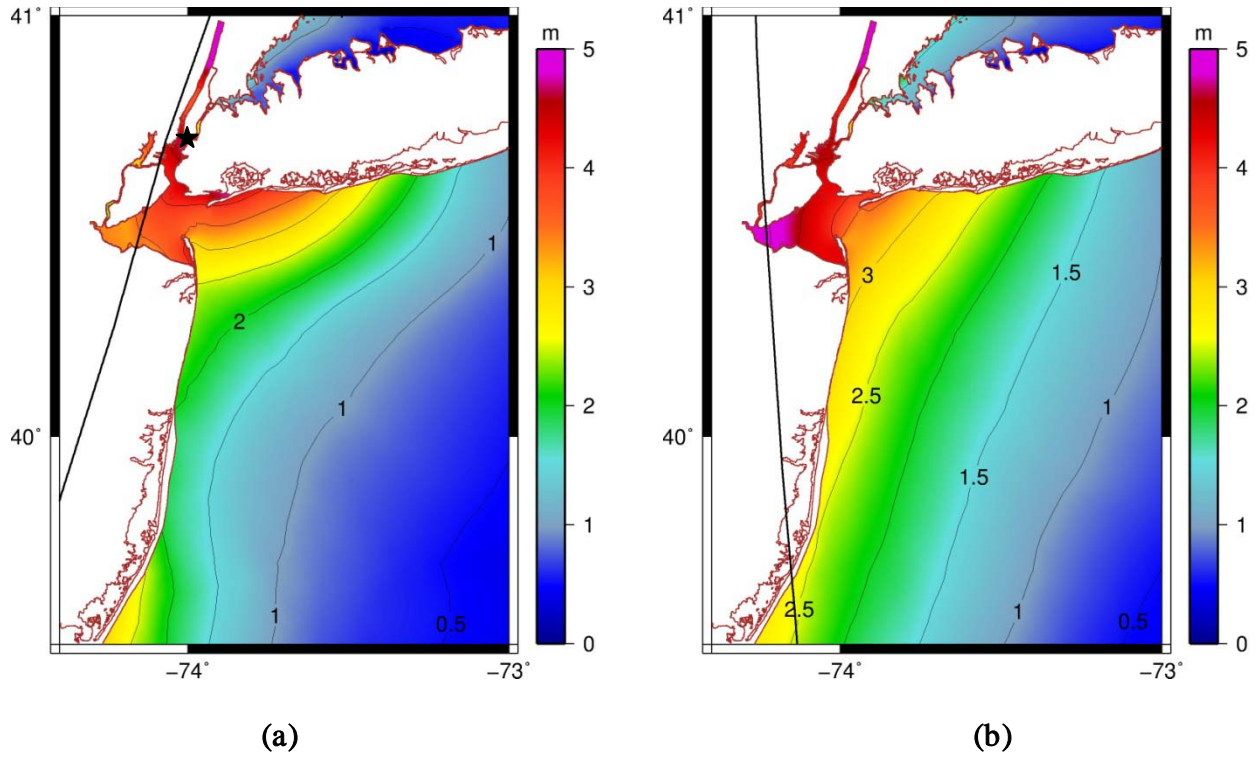
343 **Acknowledgments** N.L. was supported by the NOAA Climate and Global Change Postdoctoral
344 Fellowship Program, administered by the University Corporation for Atmospheric Research, and
345 the Princeton Environmental Institute and the Woodrow Wilson School of Public and
346 International Affairs for the Science, Technology and Environmental Policy (STEP) fellowship.
347 We thank Professor Joannes Westerink and Dr. Seizo Tanaka of the University of Notre Dame
348 for their great support on the ADCIRC implementation. We also thank Professor Brian Colle of
349 Stony Brook University for providing us with the high-resolution ADCIRC mesh.

350

351 **Author contributions** All authors contributed extensively to the work presented in this paper,
352 and all contributed to the writing, with N.L. being the lead author.

353

354 **Additional information** The authors declare no competing financial interests. Supplementary
355 information accompanies this paper on www.nature.com/nclimate. Correspondence and requests
356 for materials should be addressed to N.L. (ninglin@mit.edu).



357

358

359

360

361

362

363

364

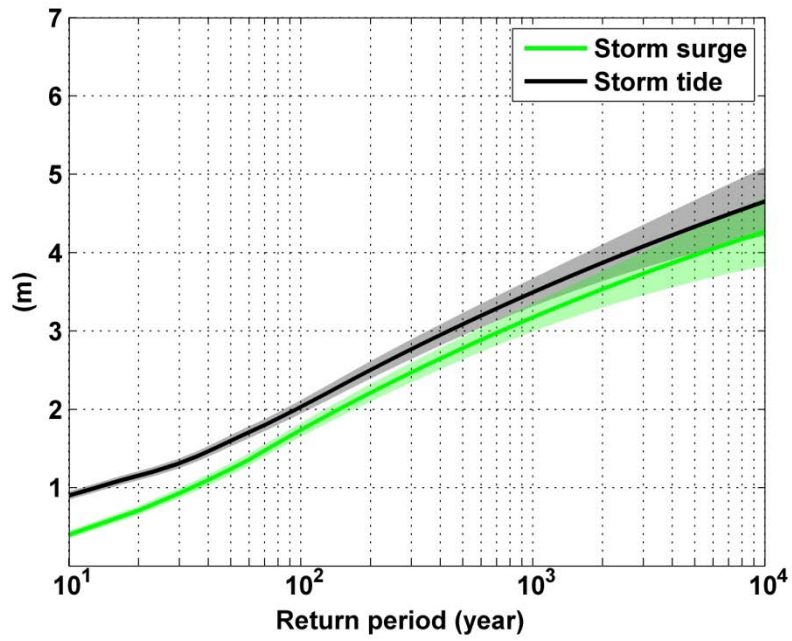
365

366

367

368

Figure 1. Two worst-case surge events for the Battery (generated by the ADCIRC simulations with resolution of ~ 100 m around NYC), under the NCAR/NCEP current climate. The contours and colors show the maximum surge height (m) during the passage of the storm. The black curve shows the storm track. The black star shows the location of the Battery. The storm parameters when the storm is closest to the Battery site are: (a). storm symmetrical maximum wind speed $V_m = 56.6$ m/s, minimum sea-level pressure $P_c = 960.1$ mb, radius of maximum wind $R_m = 39.4$ km, translation speed $U_t = 15.3$ m/s, and distance to the site $ds = 3.9$ km; (b). $V_m = 52.1$ m/s, $P_c = 969.2$ mb, $R_m = 58.9$ km, $U_t = 9.7$ m/s, and $ds = 21.1$ km.



369

370 Figure 2. Estimated return levels for the Battery of the storm surge (m; green) and storm tide (m;
371 black) for the NCAR/NCEP current climate. The shade shows the 90% confidence interval.

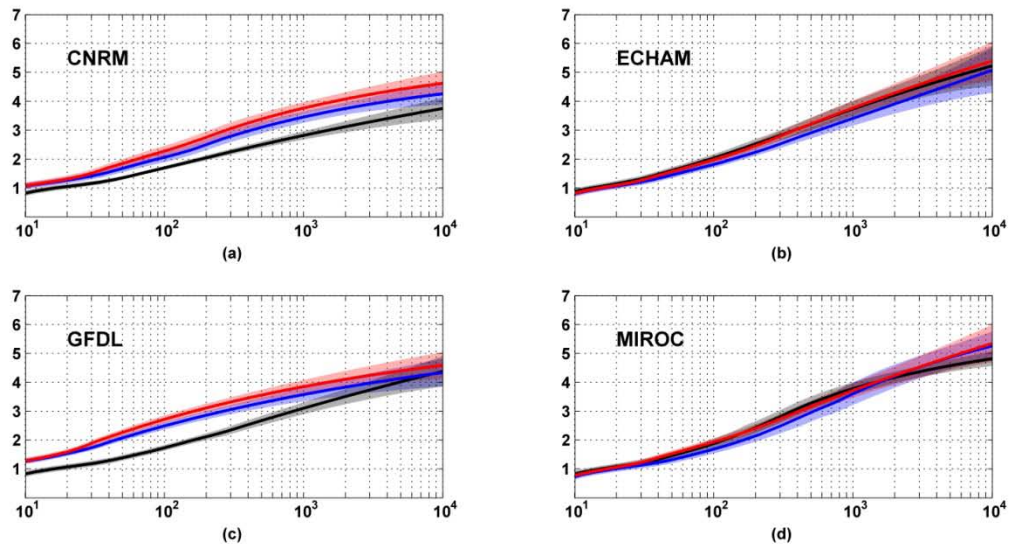
372

373

374

375

376



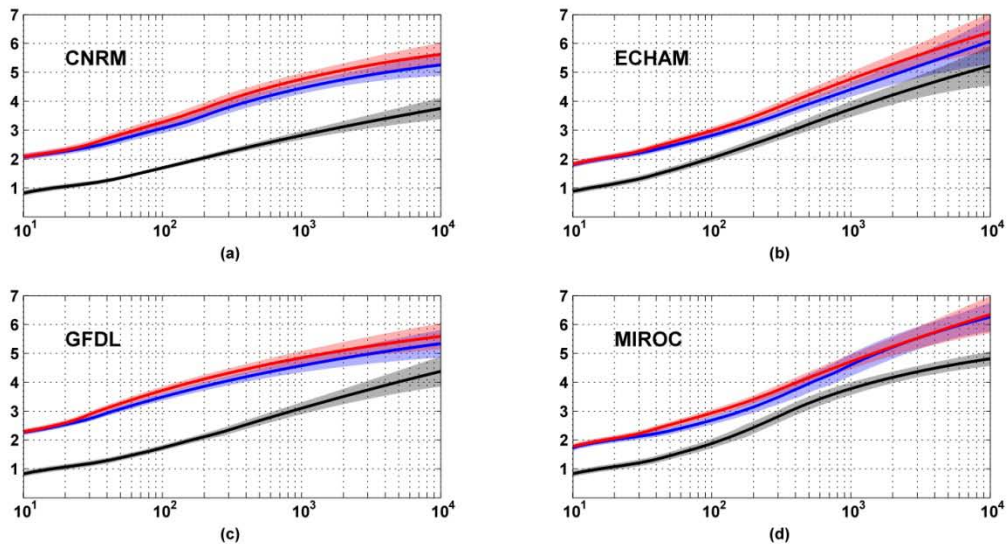
377

378

379 Figure 3. Estimated storm tide return levels for the current climate (black), the IPCC A1B
 380 climate (blue), and the IPCC A1B climate with R_o increased by 10% and R_m by 21% (red),
 381 predicted by each of the four climate models. The x axis is the return period (year) and the y axis
 382 is the storm tide (m) at the Battery. The shade shows the 90% confidence interval.

383

384



385

386

387 Figure 4. Estimated flood return levels for the current climate (black), the IPCC A1B climate
 388 (blue), and the IPCC A1B climate with R_o increased by 10% and R_m by 21% (red), predicted by
 389 each of the four climate model. The SLR for the A1B climate is assumed to be 1 m. The x axis
 390 is the return period (year) and the y axis is the flood height (m) at the Battery. The shade shows
 391 the 90% confidence interval.

392

393

394

395

396

397

¹ Emanuel, K. The dependence of hurricane intensity on climate. *Nature*, **326**, 2, 483-485 (1987).

² Emanuel, K. The hurricane–climate connection. *Bull. Am. Meteorol. Soc.* **5**, ES10–ES20 (2008).

³ Bender, M. A. et al. Model impact of anthropogenic warming on the frequency of intense Atlantic hurricanes. *Science*, **327**, 454–458 (2010).

⁴ Knutson, T. R. et al. Tropical cyclones and climate change. *Nature Geosci.*, **3.3**, 157-163 (2010).

⁵ Powell, M. D. & Reinhold, T. A. Tropical cyclone destructive potential by integrated kinetic energy. *Bull. Amer. Meteor. Soc.*, **88**, 513–526 (2007).

⁶ Resio, D.T. & Westerink, J. J. Hurricanes and the physics of surges. *Physics Today*, **61**, 9, 33-38 (2008).

⁷ Rego, J. L. & Li, C. On the importance of the forward speed of hurricanes in storm surge forecasting: A numerical study. *Geophys. Res. Lett.*, **36**, L07609 (2009).

doi:10.1029/2008GL036953

⁸ Irish, J. L. & Resio, D. T. A hydrodynamics-based surge scale for hurricanes. *Ocean Eng.*, **37**, 1, 69-81 (2010).

⁹ Irish, J. L., Resio, D.T. & Ratcliff, J.J. The Influence of storm size on hurricane surge. *J. Phys. Oceanogr.*, **38**, 2003–2013 (2008). doi: 10.1175/2008JPO3727.1

¹⁰ Resio, D.T., Irish, J.L. & Cialone, M.A. A surge response function approach to coastal hazard assessment – part 1: basic concepts. *Natural Hazards*, **51**, 1, 163-182 (2009). doi: 10.1007/s11069-009-9379-y

¹¹ Irish, J. L., Resio, D.T. & Ratcliff, J.J. The Influence of Storm Size on Hurricane Surge. *J. Phys. Oceanogr.*, **38**, 2003–2013 (2008), doi: 10.1175/2008JPO3727.1.

¹² Knutson, T.R, Sirutis, J.J., Garner, S.T., Held, I.M. & Tuleya, R.E. Simulation of the recent multidecadal increase of atlantic hurricane activity using an 18-km-grid regional model. *Bull. Am. Meteorol. Soc.*, **88**, 1549–1565 (2007). doi:10.1175/BAMS-88-10-1549

¹³ Knutson, T.R, Sirutis, J.J., Garner, S.T., Vecchi, G.A. & Held, I.M. Simulated reduction in Atlantic hurricane frequency under twenty-first-century warming conditions. *Nat. Geosci.*, **1**, 359–364 (2008). doi:10.1038/ngeo202

-
- ¹⁴ Nicholls, R.J. Coastal megacities and climate change. *GeoJournal*, **37**, 3, 369-379 (1995). doi: 10.1007/BF00814018
- ¹⁵ Rosenzweig, C. & Solecki, W. Chapter 1: New York City adaptation in context. *Ann. N.Y. Acad. Sci.*, **1196**, 19-28 (2010). doi: 10.1111/j.1749-6632.2009.05308.x
- ¹⁶ Rosenzweig, C., Solecki, W., Hammer, S.A. & Mehrotra, S. Cities lead the way in climate-change action. *Nature*, **467**, 909–911 (2010). doi:10.1038/467909a
- ¹⁷ Emanuel, K., Ravela, S., Vivant, E. & Risi, C. A Statistical deterministic approach to hurricane risk assessment. *Bull. Amer. Meteor. Soc.*, **87**, 299-314 (2006).
- ¹⁸ Emanuel, K., Sundararajan, R. & Williams, J. Hurricanes and global warming: results from downscaling IPCC AR4 simulations. *Bull. Am. Meteor. Soc.*, **89**, 347–367 (2008).
- ¹⁹ Emanuel, K., Oouchi, K., Satoh, M., Hirofumi, T. & Yamada, Y. Comparison of explicitly simulated and downscaled tropical cyclone activity in a high-resolution global climate model. *J. Adv. Model. Earth Sys.*, **2**, 9 (2010). doi:10.3894/JAMES.2010.2.9
- ²⁰ Kalnay, E. et al. The NCEP/NCAR 40-year reanalysis project. *Bull. Amer. Meteor. Soc.*, **77**, 437-471 (1996).

²¹ Solomon, S. et al., Eds. *Climate Change 2007: The Physical Science Basis*. (Cambridge University Press, 2007).

²² Jarvinen, B. R., Neumann, C. J. & Davis, M. A. S. A Tropical Cyclone Data Tape for the North Atlantic Basin, 1886–1983: Contents, Limitations, and Uses. NOAA Tech. Memo NWS NHC 22 (NOAA/Tropical Prediction Center, Miami, Fla. 1984).

²³ Villarini, G., Vecchi, G.A., Knutson, T. R., Zhao, M., Smith, J. A. North Atlantic Tropical Storm Frequency Response to Anthropogenic Forcing: Projections and Sources of Uncertainty. *J. Climate*, **24**, 3224–3238 (2011). doi: 10.1175/2011JCLI3853.1

²⁴ Luettich R.A., Westerink, J.J. & Scheffner, N.W. *ADCIRC: An Advanced Three-dimensional Circulation Model for Shelves, Coasts and Estuaries, Report 1: Theory and Methodology of ADCIRC-2DDI and ADCIRC-3DL*. DRP Technical Report DRP-92-6. (Department of the Army, US Army Corps of Engineers, Waterways Experiment Station, Vicksburg, MS, 1992).

²⁵ Westerink, J.J., Luettich, R.A., Blain, C.A. & Scheffner, N.W. *ADCIRC: An Advanced Three-Dimensional Circulation Model for Shelves, Coasts and Estuaries; Report 2: Users Manual for ADCIRC-2DDI*. (Department of the Army, US Army Corps of Engineers, Washington D.C., 1994).

²⁶ Jelesnianski, C. P., Chen, J. & Shaffer, W. A. *SLOSH: Sea, lake, and Overland Surges from Hurricanes*. (NOAA Tech. Report NWS 48, 1992).

²⁷ Jarvinen, B. R. and Lawrence, M. B. Evaluation of the SLOSH storm-surge model. *Bull. Am. Meteor. Soc.*, **66**, 11, 1408-1411 (1985).

²⁸ Jarvinen, B. & Gebert, J. *Comparison of Observed versus SLOSH Model Computed Storm Surge Hydrographs along the Delaware and New Jersey Shorelines for Hurricane Gloria, September 1985*. (U.S. Department of Commerce, National Hurricane Center, Coral Gables, FL, 1986).

²⁹ Westerink, J. J., et al. A basin- to channel-scale unstructured grid hurricane storm surge model applied to southern Louisiana. *Mon. Weather Rev.*, **136**, 833-864 (2008).
doi:10.1175/2007MWR1946.1

³⁰ Colle, B. A. et al. New York City's vulnerability to coastal flooding. *Bull. Am. Meteorol. Soc.*, **89**, 829-841 (2008). doi:10.1175/2007BAMS2401.1

³¹ Lin, N., Smith, J. A., Villarini, G., Marchok, T. P. & Baeck, M. L. Modeling extreme rainfall, winds, and surge from Hurricane Isabel (2003). *Wea. Forecasting*, **25**, 1342–1361 (2010). doi: 10.1175/2010WAF2222349.1

³² Dietrich J.C. et al. Modeling hurricane waves and storm surge using integrally-coupled, scalable computations. *Coast. Eng.*, **58**, 1, 45-65 (2011).

-
- ³³ Emanuel, K. & Rotunno, R. Self-Stratification of tropical cyclone outflow. Part I: Implications for storm structure. *J. Atmos. Sci.*, in press (2011).
- ³⁴ Georgiou, P.N., Davenport, A.G. & Vickery, B.J. Design windspeeds in regions dominated by tropical cyclones. *J. Wind Eng. Ind. Aerodyn.*, **13**, 139–159 (1983).
- ³⁵ Bretschneider, C.L. A non-dimensional stationary hurricane wave model. *Proceedings of the Offshore Technology Conference, Houston, Texas, I*, 51–68 (1972).
- ³⁶ Holland, G.J. An analytic model of the wind and pressure profiles in hurricanes. *Mon. Weather Rev.*, **108**, 1212-1218 (1980).
- ³⁷ Scileppi, E. & Donnelly, J. P. Sedimentary evidence of hurricane strikes in western Long Island, New York. *Geochem. Geophys. Geosyst.* **8**, 1–25 (2007)
- ³⁸ Coles, S. *An Introduction to Statistical Modeling of Extreme Values*. (Springer, London, 2001).
- ³⁹ Lin, N., Emanuel, K. A., Smith, J. A. & Vanmarcke, E. Risk assessment of hurricane storm surge for New York City. *J. Geophys. Res.*, **115**, D18121 (2011). doi:10.1029/2009JD013630
- ⁴⁰ Rosenzweig, C., & Solecki W. (Eds.) *Climate Risk Information, Report for the New York City Panel on Climate Change*. (Columbia Earth Inst, New York, 2009).

-
- ⁴¹ Colle, B. A., Rojowsky, K. and Buonaiuto, F. New York City storm surges: Climatology and analysis of the wind and cyclone evolution. *J. Appl. Meteor. and Climatology*, **49**, 85-100 (2010).
- ⁴² Chavas, D. R. & Emanuel, K. A. A QuikSCAT climatology of tropical cyclone size. *Geophys. Res. Lett.*, **37**, L18816 (2010). doi:10.1029/2010GL044558
- ⁴³ Emanuel, K. A. An air-sea interaction theory for tropical cyclones. Part I: Stady-state maintenance. *J. Atmos. Sci.*, **43**, 585-605 (1986).
- ⁴⁴ Emanuel, K. Environmental Factors Affecting Tropical Cyclone Power Dissipation. *J. Climate*, **20**, 5497–5509 (2007). doi: 10.1175/2007JCLI1571.1
- ⁴⁵ Gornitz, V., Couch, S. & Hartig, E. K. Impacts of sea level rise in the New York City metropolitan area. *Global and Planet. Change* **32**, 1, 61-88 (2001).
- ⁴⁶ Yin, J., Schlesinger, M.E. & Stouffer, R.J. Model projections of rapid sea-level rise on the northeast coast of the United States. *Nature Geosci.*, **2**, 262-266 (2009).
- ⁴⁷ Horton, R., Gornitz, V., and Bowman M. Chapter 3: Climate observations and projections. *Ann. N.Y. Acad. Sci.*, **1196**, 41-62 (2010).
- ⁴⁸ Hunter, J. Estimating sea-level extremes under conditions of uncertain sea-level rise. *Climatic Change*, **99**, 331-350 (2010).

⁴⁹ Mousavi, M. E., Irish, J. L., Frey, A.E., Olivera, F. & Edge, B. L. Global warming and hurricanes: the potential impact of hurricane intensification and sea level rise on coastal flooding. *Climatic Change*, **104**, 3-4, 575-597 (2010). doi: 10.1007/s10584-009-9790-0

⁵⁰ Hoffman, R. N. et al. An estimate of increases in storm surge risk to property from sea level rise in the first half of the twenty-first century. *Wea. Climate Soc.*, **2**, 271–293 (2010). doi: 10.1175/2010WCAS1050.1